Real-time Skyrme TDHF dynamics of giant resonances

Takashi Nakatsukasa [a] and Kazuhiro Yabana[a]

[a]Institute of Physics and Center for Computational Sciences, University of Tsukuba, Tsukuba 305-8571, Japan

Nuclear dynamics of giant resonances are investigated with the real-time Skyrme TDHF method. The TDHF equation is explicitly linearized with respect to variation of single-particle wave functions. The time evolution of transition densities are calculated for giant dipole resonances. The time-dependent densities of protons and neutrons suggest that the dynamics of giant dipole resonance in neutron-rich nuclei are significantly different from that in stable nuclei with $N \approx Z$.

1. Introduction

Atomic nuclei exhibit a variety of collective modes of excitation. In particular, the giant resonances always have been of central interest in nuclear structure and reaction studies. The giant resonances correspond to the most fundamental oscillations in nuclei, in the sense that they exhaust major portions of the energy-weighted sum-rule values and that the nucleus strongly absorbs energy from an external field, acting as a whole. Indeed, the giant resonances can be qualitatively described in terms of semiclassical hydrodynamical models [1].

Among many kinds of giant resonances, the isovector giant dipole resonance (GDR) is the most famous and exhausts almost 100 % of the sum-rule value. It is well explained by ordinary hydrodynamical models. This is rather exceptional because quantitative description of other modes requires a treatment as a Fermi liquid [1]. There are two famous hydrodynamical models for GDR: the Goldhaber-Teller (GT) model [2] and the Steinwedel-Jensen (SJ) model [3]. The GT model predicts $A^{-1/6}$ dependence of the GDR frequencies which arises from the concept that the restoring force is proportional to the nuclear surface area. In contrast, the SJ model relaxes the assumption of incompressibility, which leads to $A^{-1/3}$ dependence of the GDR frequencies. Experimental data are best fitted by a combination of these two [4]: In light nuclei, the data seem to indicate the $A^{-1/6}$ law, while the $A^{-1/3}$ dependence becomes increasingly dominant for increasing values of A.

The hydrodynamical models have a close connection to the time-dependent Hartree-Fock (TDHF) theory. In the limit of $\hbar \to 0$, the TDHF equation goes over into the Vlasov equation. Therefore, without the collision term, the TDHF should provide a microscopic description of an appropriate hydrodynamical model. Recently, we have proposed the real-time TDHF method combined with the absorbing-boundary condition (TDHF+ABC method) for a linear response function [5,6]. This may be regarded as an extension of the

continuum random-phase approximation (RPA), made applicable to a deformed system. In this paper, we show real-time dynamics of the TDHF for GDR and discuss how their properties change from stable ($N \approx Z$) to unstable nuclei ($N \gg Z$). As is discussed in the following sections, we take a small-amplitude limit of the TDHF. Although this is equivalent to the RPA, the time-dependent snap shots of the TDHF wave packet may provide an intuitive dynamical picture of the GDR. It should be also noted that the TDHF provides a proper description for low-lying modes as well, for which quantum effects are so important that the semiclassical hydrodynamical models are not applicable.

2. Linearized TDHF in real time

The HF ground state is assumed to be a Slater determinant which consists of A single-particle orbitals, $\Phi_0(x_1, \cdots, x_A) = \det\{\phi_i(x_j)\}_{i,j=1,\cdots,A}$ with $x = (\vec{r}, \sigma, \tau)$. Each single-particle orbital is determined by

$$h[\phi, \phi^*]\phi_i(x) = \epsilon_i \phi_i(x) \qquad \text{for } i = 1, \cdots, A, \tag{1}$$

where $h[\phi, \phi^*]$ is the single-particle Hamiltonian which depends on $\phi_i(x)$ $(i = 1, \cdots, A)$ self-consistently. The TDHF equation is obtained by replacing, in Eq. (1), ϵ_i by the time derivative $i\hbar\partial/\partial t$, and $\phi_i(x)$ by the time-dependent wave function $\psi_i(x,t)$. The TDHF equation is now linearized with respect to variation of each single-particle wave function and a time-dependent external field $v(x,t)$. Substituting $\psi_i(x,t) = (\phi_i(x) + \delta\psi_i(x,t))e^{-i\epsilon_i t/\hbar}$ into the TDHF equation, we have

$$i\hbar\frac{\partial}{\partial t}\delta\psi_i(x,t) = \left(h[\phi, \phi^*] - \epsilon_i\right)\delta\psi_i(x,t) + \delta h(t)\phi_i(x) + v(x,t)\phi_i(x), \tag{2}$$

where $\delta h(t) \equiv h[\psi, \psi^*] - h[\phi, \phi^*]$ in the first order of $\delta\psi_i(x,t)$. If we put $\delta h(t) = 0$, Eq. (2) gives unperturbed particle-hole excitations with a fixed single-particle potential in $h[\phi, \phi^*]$. $\delta h(t)$ is nothing but the residual interaction in the language of the energy representation. The second term in the r.h.s. of Eq. (2) contains a dynamical effect which comes from variations of the self-consistent one-body potential.

Equation (2) is equivalent to the well-known RPA equation in the energy representation. In practice, however, there are some differences, advantages and disadvantages in each method. For instance, the uncertainty in energy, ΔE, is inversely proportional to the period of the time propagation T; $\Delta E \sim \hbar/T$. Therefore, when we want to distinguish states nearly degenerate, we need to propagate the wave functions for a long period of time. In this case, the energy representation may be a better choice. On the other hand, when we are interested in a bulk structure of excited states in a wide range of energy, calculations using the time representation becomes more efficient than those with the energy representation. The time-dependent calculation should be suitable for giant resonances, since their energies are rather high and spread over a wide range of energy.

The transition density in the time representation is defined by the density variation from its ground-state value,

$$\begin{aligned}\delta\rho(x, x'; t) &= \rho(x, x'; t) - \rho_0(x, x') \\ &= \sum_{i=1}^{A} \left\{\phi_i^*(x)\delta\psi_i(x', t) + \delta\psi_i^*(x, t)\phi_i(x')\right\}. \end{aligned} \tag{3}$$

In this paper, we are mainly interested in the spin-independent diagonal part of Eq. (3);

$$\delta\rho_\tau(\vec{r};t) = \sum_{i=1}^{A}\sum_{\sigma}\left\{\phi_i^*(x)\delta\psi_i(x,t) + \delta\psi_i^*(x,t)\phi_i(x)\right\}. \tag{4}$$

The expectation value of an operator $\hat{F}(\vec{r},\tau)$ can be expressed as

$$F(t) = F_0 + \delta F(t) = F_0 + \sum_{\tau}\int d^3r\hat{F}(\vec{r},\tau)\delta\rho_\tau(\vec{r};t), \tag{5}$$

where F_0 is the ground-state expectation value.

The external field $v(x,t)$ in Eq. (2) can be chosen according to the purpose of the calculation. In order to calculate the strength distribution in a wide range of energy, an instantaneous external field, $v(x,t) = v(x)\delta(t)$, is suitable, because this excites the system to states in all energies. In contrast, if we adopt an oscillating field with a fixed frequency ω, $v(x,t) = v(x)\cos(\omega t)$, the system is excited to a specific state with $E_{\rm x} = \hbar\omega$. In this way, we can investigate dynamical properties of the specific state in the time-dependent manner.

To calculate the strength function of the operator $\hat{F}(\vec{r},\tau)$,

$$S(\hat{F};E) = \sum_{E'}\delta(E-E')\left|\langle\Psi_{E'}|\hat{F}|\Phi_0\rangle\right|^2, \tag{6}$$

we adopt the external field $v(x)$ proportional to $\hat{F}(\vec{r},\tau)$. Then, $S(\hat{F};E)$ can be obtained as the Fourier transform of the expectation value of Eq. (5).

Before showing results, let us discuss a numerical difficulty related to presence of zero modes in nuclei. The "zero mode" means zero-energy modes of excitation associated with the spontaneous symmetry breaking in the HF states, such as translation and rotation. These modes should correspond exactly to the zero energy if the numerical calculation is perfect. However, a small numerical error and approximation may give imaginary energies to these modes. Since the time evolution of wave functions carries all the information of the excited states, the presence of these imaginary-energy modes leads to a kind of numerical instability to prevent performing a long period of the time propagation. Thus, we need to remove components of the zero modes from the time-dependent single-particle wave functions $\delta\psi_i(x,t)$. The zero modes can be constructed by operating the symmetry operator $\hat{P}$ and its conjugate one $\hat{Q}$ to the ground state. For the translational case, $\hat{P}$ is the total momentum operator and $\hat{Q}$ is the center-of-mass coordinate.

3. Giant dipole resonances in stable and neutron-rich nuclei

We now apply the method to GDR in even-even Be isotopes. We calculated $B(E1)$ distribution for Be isotopes in Ref. [6] using the SIII parameter set. We found that the large deformation splitting in ^{8}Be and ^{14}Be, because of the large quadrupole (prolate) deformation in the ground state ($\beta_2 \approx 0.8$). However, the width in ^{14}Be is much larger than that in ^{8}Be. These results are robust and do not depend on the choice of the Skyrme parameter set. We also found that there is a significant low-energy $E1$ strength around $E_{\rm x} = 5$ MeV for ^{14}Be [6]. However, the $E1$ strength and its peak position are rather

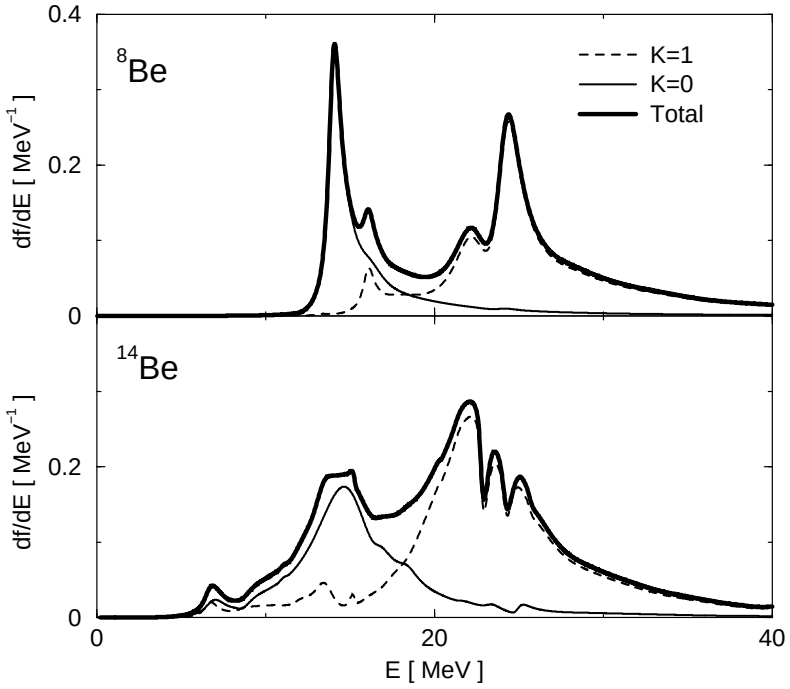

Figure 1. Calculated $E1$ oscillator strength distribution in ^{8,14}Be. Thin solid and dashed lines indicate the response to dipole fields parallel and perpendicular to the symmetry axis, respectively. Thick line shows the total strength.

sensitive to the choice of the parameters. Thus, in this section, we show time-dependent transition densities for the main peak of GDR.

The calculation is performed on the three-dimensional Cartesian coordinate grid space, using the Skyrme energy functional of Ref. [7]. The Galilean symmetry is respected in this functional including the spin-orbit, Coulomb, and time-odd densities. We adopt the SGII parameter set in the calculation. In order to take account of the single-particle continuum, we use the absorbing potential outside of the interacting region [5,6]. In Fig. 1, we show the $E1$ oscillator strength distribution for ^{8,14}Be. Two-peak structure due to the deformation splitting is prominent for both ^{8}Be and ^{14}Be. Hereafter, let us focus our discussion on the peak around $E_{\rm x} = 15$ MeV with $K = 0$.

We use a Gaussian-pulse external field, $v(x,t) = M(E1)_{K=0} \cos(\omega t) e^{-\gamma(t-t_0)^2}$, to selectively excite the GDR around $E_{\rm x} = \hbar\omega = 15$ MeV, with $\gamma = 3$ MeV/$\hbar$ and $t_0 = 2$ $\hbar$/MeV. Then, the spin-independent transition density of Eq. (4) is calculated in the 3D coordinate space. It turns out that one of the Steinwedel-Jensen's assumptions, $\delta\rho_n(\vec{r};t) = -\delta\rho_p(\vec{r};t)$, is approximately satisfied for ^{8}Be. In contrast, in ^{14}Be, we see a large deviation from this property. Figure 2 shows how $\delta\rho_\tau(\vec{r},t)$ ($\tau = p, n$) evolve in time in the x-z plane. The time difference from one panel to the next is $\Delta t = 0.2$ $\hbar$/MeV which roughly corresponds to the half period π/ω. We see that significant portions of neutrons actually move together with protons. The neutron transition density $\delta\rho_n$ shows a peculiar node structure. In Fig. 2, the regions of $\delta\rho_p > 0$ ($\delta\rho_p < 0$) have a large overlap with the those of $\delta\rho_n > 0$ ($\delta\rho_n < 0$).

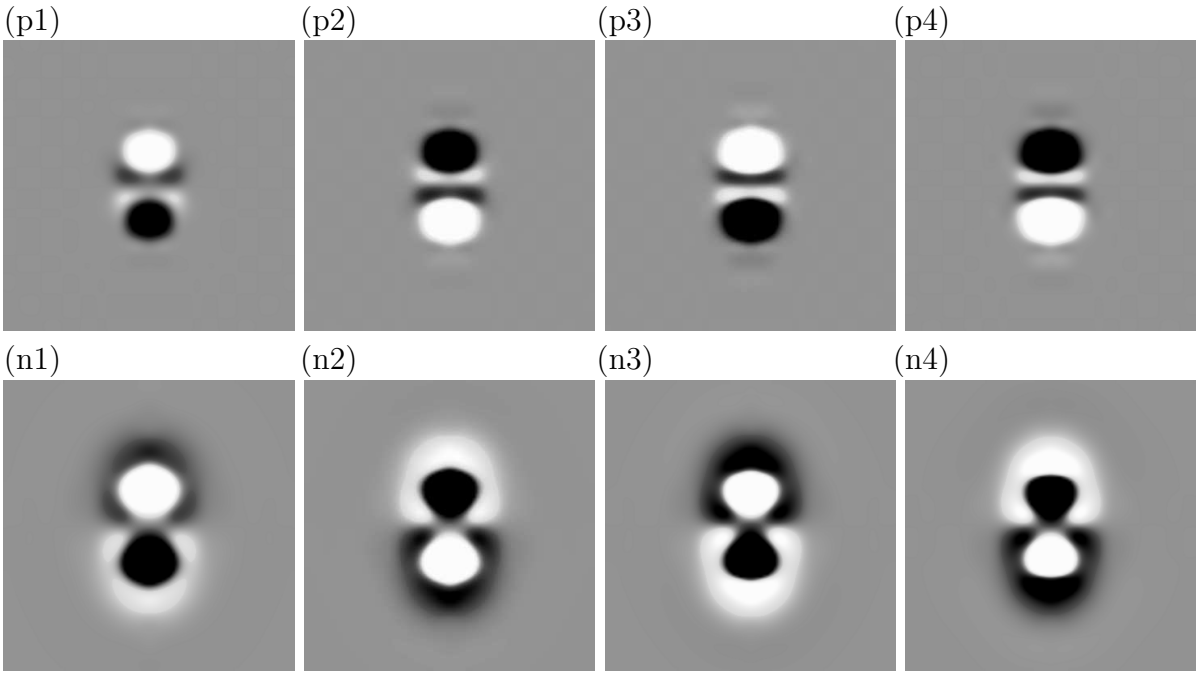

Figure 2. Snap shots of calculated $\delta\rho_\tau(\vec{r},t)$ in the x-z plane for the $K=0$ peak at $E_{\rm x}=15$ MeV in ^{14}Be. The upper panels (p1-4) indicate $\delta\rho_p(\vec{r};t)$, while the lower (n1-4) for $\delta\rho_n(\vec{r};t)$. White (black) regions indicate those of $\delta\rho_\tau>0$ ($\delta\rho_\tau<0$). The time difference between two neighboring panels is $\Delta t=0.2$ $\hbar$/MeV. The two panels at the same column corresponds to the same time t.

This means a violation of the property of the SJ model, $\delta\rho_p+\delta\rho_n=0$. Weakly bound neutrons in neutron-rich nuclei seem to be significantly affected by strong attraction between protons and neutrons, and to oscillate in phase with protons' movement. This is a consequence of the dynamical effect of the time-dependent self-consistent potential, $\delta h(t)$ in Eq. (2).

4. Summary

We present calculations of the linearized TDHF method in real time for giant dipole resonances in ^{8,14}Be. These nuclei are calculated to be largely deformed in the ground state. The main GDR peak is split into two peaks with $K=0$ and $K=1$. We show the time-dependent transition densities for $K=0$ peaks. The total density, $\rho_p+\rho_n$, is approximately conserved for ^{8}Be, while its conservation is significantly violated in ^{14}Be. The time evolution of the transition density, $\delta\rho_\tau(t)$, suggests a strong dynamical effect for neutron-rich nuclei, and seems to indicate the mixture of the isoscalar volume-type and the isovector surface-type components.

This work has been supported by the Grant-in-Aid for Scientific Research in Japan (Nos. 17540231 and 17740160). The numerical calculations have been performed at SIPC, University of Tsukuba, at RCNP, Osaka University, and at YITP, Kyoto University.

REFERENCES

1. P. Ring and P. Schuck, *The Nuclear Many-Body Problem* (Springer-Verlag, New York, 1980).
2. M. Goldhaber and E. Teller, Phys. Rev. **74** (1948) 1046.
3. H. Steinwedel and J. H. D. Jensen, Z. Naturforschung **5A** (1950) 413.
4. B. L. Berman and S. C. Fultz, Rev. Mod. Phys. **47** (1975) 713.
5. T. Nakatsukasa and K. Yabana, J. Chem. Phys. **114** (2001) 2550.
6. T. Nakatsukasa and K. Yabana, Phys. Rev. C **71** (2005) 024301.
7. P. Bonche and H. Flocard and P. H. Heenen, Nucl. Phys. A **467** (1987) 115.